# Non-linear blast responses of thin shell roof over long span structures

Rennie, Jake; Kaewunruen, Sakdirat; Baniotopoulos, Charalampos

Link to publication on Research at Birmingham portal

# Non-linear blast responses of thin shell roof over long span structures

**Jake Rennie, MEng (First Class)**

Email: jake@d-engine.co.uk

Design Engine

5th Floor, East Wing, Trinity Point

New Road, Halesowen B63 3HY


**Dr Sakdirat Kaewunruen, BEng (Hons), MEng, PhD, MBA, FIEAust, CPEng, NER, RPEQ, FHEA**

Email: s.kaewunruen@bham.ac.uk

Department of Civil Engineering

The University of Birmingham

Edgbaston, Birmingham B15 2TT


**Professor Charalampos Baniotopoulos, PhD, CEng**

Email: C.Baniotopoulos@bham.ac.uk

Department of Civil Engineering

The University of Birmingham

Edgbaston, Birmingham B15 2TT

**Abstract**

This paper adopts both explicit and implicit finite element methods in a specialist package LS-DYNA to investigate the non-linear, dynamic response of a long span shell roof structure when subjected to blast loading. Parametric studies have been carried out on blast loaded laminated glass plates with reference to experimental results obtained by European researchers. A case study that has been chosen is a light rail station in The Netherlands called The Erasmusline. Following the detonation of 15kg TNT charge, explicit analysis showed breakage surrounding the rigid supports along the edge beam where modal vibrations are restrained. An implicit analysis has confirmed the resonances in global eigen-frequencies where most blast damage is localised around the roof canopy hence producing cracking and potential glass detachment from the panels without full structural demolition. This insight from this study will inform structural engineers about the potential modes of failure and preventative strategies to minimise further secondary losses of life or assets from a terrorist attack.

**Keywords**

Finite element modelling, materials technology, shell structures, blast effect, nonlinear response

**List of notation**

$p(t)$ – Pressure-time function

$p_0$ – Atmospheric pressure

$p_{max}$ – Peak pressure

$t_d$ – Time spent in the positive phase (before crosses x-axis)

$t$ - time

$b$ – blast constant

$Z$ – Scaled Distance

$R$ -- Distance

$W$ – Charge weight


## 1.0 Introduction

Design against blast loading is an ongoing and vital research subject in structural engineering. This is a direct result of the constant threat of terrorism around the globe; infrastructure posing a significant risk appears to be associated with the public transportation system where the potential for mass disruption and destruction is greatest (Larcher et al., 2015). A study conducted by The National Consortium for the Study of Terrorism and Responses to Terrorism (2016) stated that 89 terrorist attacks were targeted at the transportation system sector between 1970 and 2015 in America. These statistics are able to bolster the research into blast resistant design in critical infrastructure. Modern technologies have allowed architecture to produce elegant, slender structures that optimise the use of space in very compact environments such as cities. These constraints lend themselves to the utilisation of thin shells, which derive their strength from their shape and are known as form resistant structures (Ter Maten, 2011). The application of thin shells maximise the efficiency of construction materials through membrane theory where out of plane forces are able to be resisted by in plane responses (Blaauwendraad and Hoefakker, 2014). The compromise between blast resistance and structural slenderness is ongoing with further advancements having been made in blast resistant glass.

This paper investigates the dynamic response of curved glass when subjected to blast pressures. The expulsion of glass panes has previously been considered beneficial in order to relieve internal pressures; however the fragments can cause more damage as they shower down on the public and infrastructure below (British Gas Corporation, n.d.). An example of this is in the 1995 Oklahoma City bombing: 198 people suffered direct glass related injuries such as lacerations or abrasions from flying glass debris, a further 265 people suffered hearing impairment from the blast where glass windows were shattered and no longer able to exhibit their acoustic insulation properties (Zhang, Hao and Ma, 2013). Glazing and structural technologies are being revised to prevent these phenomena and will be discussed further in this section.

2

Thin shells can be dated back to the Roman Empire where Byzantium architecture utilised this doubly curved geometry to maximise a material's structural capabilities (Coskun, 2016). With the advancement of modern technologies, shell design is becoming more popular in the structural engineering field. Theories proposed by Bernoulli, Euler, Kirchhoff and Love in the 1800's have been adopted and modified to account for modern materials, by applying the methods of continuum mechanics e.g. the theory of elasticity of three-dimensional bodies (Mollmann, 1981). Despite these advancements, computational methods can prove difficult due to the non-linearities associated with the material and blast dynamics, where under large strains the material no longer exhibits elasticity (Subramani and Sugathan, 2012).

Explosion resistant design is becoming a major design parameter, particularly when designing high risk infrastructure such as train stations. With modern construction using glass due to its sustainable benefits of natural light and insulation, significant research has been conducted into blast resistant glazing design. A traditional theory in this design process would be that the glass would simply disintegrate upon blast loading, relieving the pressure and causing no further damage. Nowadays, significant advancements cause glass fragments to stay attached to the structure saving lives and money. Toughened glass has been heat treated to instil differential stresses in each pane, causing the glass to shatter into small shards upon fracture This glazing is a major advancement to annealed glass that will fracture into large pieces causing catastrophic damage when travelling at high velocities. Laminated glass attempts to retain these glass fragments by utilising an adhesive polyvinyl butyral (PVB) interlayer. The addition of this layer enables the laminate to sustain large, non-linear strains to further absorb the blast energy (Fam and Rizkalla, 2006).

Laminated glass benefits from improved cross-sectional moduli owing to its increased thickness with further improvements in the glass' fracture strength when compared to its monolithic equivalent (Hooper et al., 2012). Figure 1 shows the stress distribution of the laminated glass as failure occurs across the laminate. As the glass cracks, no tensile strength can be exhibited and complete failure occurs when the interlayer tears as shown in figure 1d. This study aims to investigate the full composite behaviour under blast which includes the hyperplastic non-linear capabilities of the interlayer.
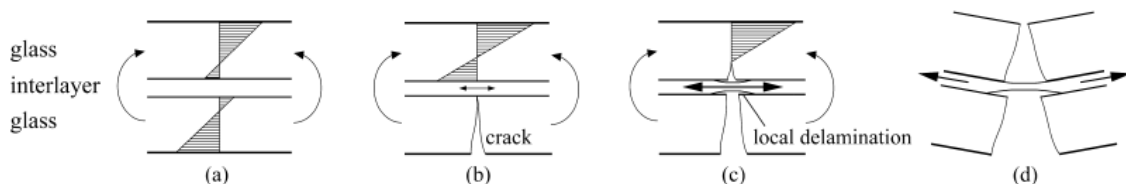


**Figure 1: Cross-sectional response of laminated glass subjected to blast (Pelfrene et al., 2016)**
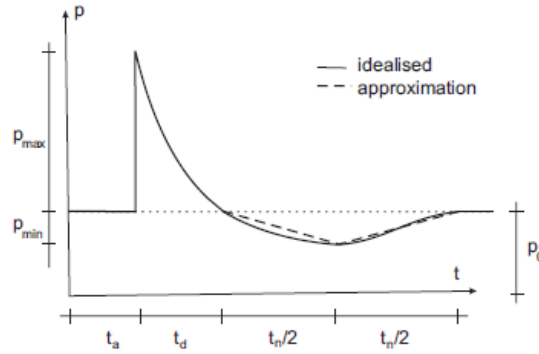
**Figure 2: Blast pressure evolution (Larcher et al., 2011)**

Research conducted by Larcher et al., (2011) explains the pressure evolution of a blast wave when propagating through an Eulerian fluid; the pressure plot can be seen in figure 2. The rapid release of energy propagating from the blast centre results in a sudden increase in pressure, this overpressure will diminish and drop below atmospheric to begin the negative phase of loading. The loading action shown in Figure 2 is a function of both charge weight and stand-off distance based on Equation 2, and will be used as validation for the finite element results. Research has shown that much more work has been conducted on the positive phase when, in fact, just as much damage can be caused by the negative phase especially when the initial overpressure has produced cracking in the outer fibres, this research has been conducted by Dharani and Wei (2004) and can be found later in this paper. The shape of the pulse can be modelled using the Friedlander equation (1) however this impulse can be greatly affected by the built environment which can cause reflections and superposition reaching reflected waves of up to 14 times the incident peak (Larcher et al., 2011).

$$p(t) = p_0 + p_{max}(1 - \frac{t}{t_d})^{-\frac{bt}{t_d}} \tag{1}$$

With thin shells becoming a more frequent architectural device, it is important to understand the structural behaviour under blast loading; a research topic that has been seldom studied on full scale structures. A study conducted by Larcher et al. (2015) determined the blast effects inside train carriages using simple 2D solid shell elements. The fragmentation and erosion of elements as the blast propagates is what this investigation also aims to achieve, as well as to investigate the non-linear response of a structure. In this study, advanced meshing and very delicate attention to modelling materials are required to model a complex, doubly curved structure. This accuracy has been achieved in studies such as those written by Hidallana-Gamage et al. (2013) and Hoo Fatt and Sirivolu (2015) when modelling blast loaded plates, however this accuracy has yet to be translated to full-scale structures.

4

In this study, LS-DYNA will be used to simulate an explosion at platform level of a light-rail station in the Netherlands. This package is capable of running computational fluid dynamics alongside computational solid mechanics to explore its structural response (Ngo et al., 2007). Due to the dynamic nature of the loading and the complex geometries of the roof structure, simple, linear analysis cannot be used. Non-linear transient analysis will therefore be employed. LS-DYNA is capable of this method of analysis and can provide accurate results providing the user understands the equations of state, solvers, fluid-structure interaction, meshing, etc. (Hilding, 2016). The scope of this study is to computationally model the non-linear effect of blast on a long span shell structure using explicit and implicit finite element methods in LS-DNYA. The parametric studies will be carried out in order to investigate the transient-dynamics of the blast pulse in the atmosphere, and the effects of rigid bodies surrounding the charge. This study highlight new research into material models, meshes and solvers used in LS-DYNA to accurately simulate the blast effect on laminated glass. The case study has been carried out to demonstrate nonlinear responses of the entre glass canopy as well as singular glass sheets.

## 2.0 Previous studies into blast effects

LS DYNA offers a vast database of parameters that combine to form a model best suited to certain scenarios. For glass, recurring formulations have been researched to attempt to accurately model its response to blast. Table 1 shows some combinations used in previous studies when modelling a simple glass plate. A frequent problem with each of these studies is the computational power that each one demands due to the dense meshes being used. These studies have informed the numerical model used in this study.

| References | 2D/3D | Material models / Element's properties | Technical discussion |
|---|---|---|---|
| Deng and Jin (2010) | 3D | Glass: eight node, Lagrangian hexahedron elements with one integration point. Glass ply modelled as linear elastic, core modelled as viscoelastic Air/fluid: MM-ALE blast strategy | 272,797 elements and 477,045 nodes were modelled, and hence super computer was required, processing time: 361h. Viscoelastic core modelled which is not how it responds under blast (elastoplastic) MM-ALE strategies very computationally expensive due to entire domain meshing. |
| Hidallana-Gamage et al. (2013) | 3D | Glass: material model 110 Core: Material model 24 (elastoplastic) | Material model 110 takes in to account fracture strength of glass, model 24 accounts for high strain rates. 3D modelling can be expensive. |

| Hidallana-Gamage et al. (2013) | 2D | Material model 32 with 10 integration points | Material model 32 allows for failure criteria to be defined in the glass however this criterion cannot be applied to the interlayer and thus complete failure cannot occur. 2D requires less processing power. |
|---|---|---|---|
| Zhang, Hao and Ma (2013). | 3D | 8 node (fully integrated), SOLID164 element used for glass and interlayer, JH2 model, | Fully integrated to allow for lack of through thickness of glass, without compromising processing power. JH2 model to account for high strain rate and potential material damage/cracking |

**Table 1: LS-DYNA methods, models and solvers comparison**

A study conducted by Kaewunruen et al. (2017) investigated the effects of blast on London's Canary Wharf station. Despite attaining a model for the damage evolution of the roof when exposed to transient blast conditions, it appeared monolithic glass was modelled. In reality, the glass is double laminated and would hence have a different response when subjected to blast loading due to the presence of the polyvinyl butyral (PVB) interlayer. Monolithic glass is much easier to model as failure of the glass would occur instantaneously after cracking whereas the interlayer of a laminated glass panel would hold the fragments together and exhibit a more non-linear response until tearing occurs. Hidallana-Gamage et al. (2014) identify the limitations of previous models, most commonly associated with incorrectly modelling the PVB interlayer and how previous models don't utilise the full strains of laminated glass after cracking, seen in the study conducted by Kaewunruen et al. (2017). Experiments conducted by Cormie et al. (2009) emphasised the importance of modelling laminated glass post cracking and state that the pre-cracking strains that can be utilised are only 3% of the total strain capacity.

Kaewunruen et al. (2017) use the Von Mises stress to evaluate the damage evolution from a 6.25kg TNT charge. The results show that it takes 8ms for failure of the first panel to occur and is subsequently followed by 8 further panels breaking at 9ms. Hooper et al. (2012) yielded similar results of 9ms for full interlayer failure of a singular glass plate which shows good agreement to experimental results. Alike Kaewunruen et al. (2017), the blast wave will be modelled according to Unified Facilities Criteria (UFC). (2014) guidelines, where a surface burst causes a hemispherical blast wave to be produced due to blast wave reinforcement. The study conducted by Hidallana-Gamage et al. (2014) compares the numerical response from the LS DYNA program to the experimental results in a shock tube test. This study investigated the importance of the PVB interlayer, although accurate results were obtained, complete failure of the glass (tearing failure of the interlayer) was not observed and therefore fragmentation hasn't occurred. For completeness, and to show the full response of the glass to severe blast loading,

complete destructive testing should've been carried out and modelled, this would aid comparison against other research papers testing laminated glass to full failure.

Research conducted by Larcher et al. (2011) uses EUROPLEXUS to model 2 blast experiments: the first was conducted by Kranzer et al. (2005) and uses small charges to deflect a glass plate without interlayer failure. The second was conducted by Hooper et al. (2012) and uses large charges to investigate the full failure of the specimen. The most effective model constructed in this study used layered elements with a failure criterion to ensure the glass elements get deleted when this criterion is reached. This has been proven in many studies to effectively model the transition between the pre-crack and post-crack phases. It can however lead to instabilities as mass is not conserved in the system. Zhang, Hao and Ma (2013), further explain how erosion can lead to premature deletion if due care is not taken. Hooper et al (2012) use a somewhat user-controlled failure criterion to separate the pre and post-crack phases by assuming fracture after a principle stress of 80kPa was reached. At this point the simulation is stopped, and the glass sectional moduli are reduced to zero thus exhibiting no strength properties. The current output file database, e.g. strain, position, velocity, is then used as the input file for the post-crack phase (Hooper et al., 2012). The subsequent simulation therefore only models the interlayer with no loss of mass or energy. The assumption of the glass exhibiting zero strength is very conservative as the cracks would need to be perfectly aligned, with no contact between fragments as the glass deforms for these properties to prevail (Hooper et al., 2012). This scenario is very unlikely and therefore some strength can be shown in cracked glass.

For the case of solid structures such as concrete, the positive phase of blast is the most destructive, for this reason, ample research has been conducted on this topic. For the case of thin shell structures however the negative phase can cause just as much damage. Dharani and Wei (2004) have studied the effect of the negative phase using both empirical and finite element solutions. According to this study, the negative phase has the most destructive effect when cracking occurs in the plies to adversely affect the sectional moduli and worsen the rebound deflection. Hidallana-Gamage, Thambiratnam and Perera, (2017) however explain how this phase can be negated from the model when the support conditions are considered rigid. When the boundaries are fixed, the energy absorption, centre deflection and support reactions are negligibly affected by the inclusion of the negative phase. The gridshell structure to be modelled in this paper (see next section) uses rigid supports and can therefore disregard the negative phase to simplify the model.

Contrary to much research on laminated glass to blast loads, Dharani and Wei (2004) have also opted for the modelling of the interlayer as a viscoelastic material. PVB however has been found to respond differently under more rapid strain rates. According to Larcher et al. (2011), at rates greater than $10s^{-1}$ (approaching that of a blast) the interlayer acts as a glassy (elastic)

material and therefore modelling of a viscoelastic material would respond inaccurately in the analysis. It must be mentioned that there were 8 years between the publishing of these research papers and therefore advancements in the modelling potential of LS-DYNA could have allowed for more complex properties to be exploited.

Many studies have been carried out on the topic of modelling blast loading on simple structures using LS-DYNA; however, the application of these models to modern architecture has been seldom researched. A further knowledge gap has been identified into the non-linear response of blast loading on laminated glass thin shell structures. This paper justifies this gap and uses LS-DYNA to produce a representative model on the blast effects on long span thin shell structures, applying the model to a case study of a light rail station in the Netherlands called The Erasmusline.

### 3.0 Case study

Before any computer modelling and analysis can occur, the case study needs to be identified. The structure must be long spanning, singly/doubly curved and preferably a high-risk target for terrorism. The structure to be analysed is called The Erasmusline located in the Dutch city of The Hague and can be seen in Figure 3.
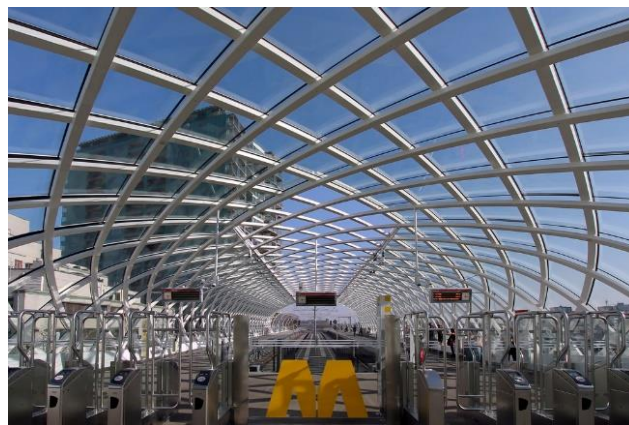


**Figure 3: The Erasmusline, The Hague, Netherlands**

The structure optimises a gridshell roof canopy with singly curved glass along platform level and double curved at the "closed end". It is 90m long and spans 17m across the platform, the maximum height above platform level is 6m and is formed of rectangular hollow sections for the mesh and cold formed laminated glass as the canopy (Helbig et al., 2016). The boundary conditions use one pinned connection on either side of the roof connecting to the edge beam to allow for the required rotation, the remaining connections are able to slide longitudinally, to allow for thermal effects (Helbig et al., 2016). The laminate construction of the roof canopy uses 10mm plies according to Helbig et al. (2016) and a (assumed) 5mm interlayer. The15kg blast

will be located in the "closed" end of the structure where the danger to both life and structure will be most catastrophic.

## 4.0 Methodology

This study aims to model both the non-linear response of the laminated glass shell panel as well as the breakage configuration of the entire structure due to blast. The former involves a single panel that is modelled similar to the research conducted by Kranzer et al. (2005) and Hooper et al. (2012) and the latter reflects the work of Kaewunruen et al. (2017), where the entire Canary Wharf underground station canopy was modelled against blast effects. It is a common approach to model laminated glass as monolithic when analysing against short term loads. This is because the interlayer behaves as a relatively stiff material in short term loads like blast (Pelfrene et al., 2016). The shear modulus of 10MPa results in bending stresses similar to that of a monolithic pane under blast loads, where these similarities end is when the glass breaks. Cracks in the glass allow the plies to only withstand compressive forces and the PVB interlayer to withstand the tensile forces until tearing occurs (Pelfrene et al., 2016). The transition of strength between the layers of the laminate throughout the stages of blast loading was an important phenomenon to attempt capture by the model.

The literature has proposed various material models that have proven successful when modelling laminated glass; it has however seldom specified the element formulations that enable the material model to perform accurately. For this reason, a parametric study aimed to inform the final case study on the entire model make up in order to model the structure as accurately as possible. The material models that will be used can be found in Table 2.

| Material number | Material | Justification |
|---|---|---|
| MAT_001 | Elastic | This informed the final study on the pre-crack behaviour of the composite as Laminated glass exhibits a linear-brittle response until cracking occurs, this was investigated by Hooper et al. (2012) |
| MAT_024 | Linear piecewise plasticity | Used by Hidallana-Gamage et al. (2013), to model elastoplasticity of the interlayer, by modelling the interlayer with solid elements, transverse shear deformations can be included which are important (Bohm, Haufe and Erhart, 2016). This material is also effective in modelling the silicone sealant joints surrounding glass plates. |
| MAT_032 | Laminated glass | This is Material Type 32. With this material model, a layered glass including polymeric layers can be modeled. Failure of the glass part is possible. Used by Larcher et al. (2011) and Hidallana-Gamage et al. (2013) as an inexpensive method of modelling the laminate. This material was |

9

| | | used with shell elements and assigns polymer or glass properties to each integration point as specified by user. When the plastic strain limit is reached, the integration points associated with glass reduce its strength moduli to zero and the deformations rely on the interlayer. |
|---|---|---|
| MAT_110 | Johnson Holmquist Ceramics | This is Material Type 110. This Johnson-Holmquist Plasticity Damage Model is useful for modeling ceramics, glass and other brittle materials. |
| | | This model represents the initiation and propagation of cracking through the introduction of damage variables (Cronin et al., n.d.), these are inputted as intact and fractured strength parameters seen in appendix A. This model has been proven effective to model the pre-instilled flaws associated with the production process. |
| | | Hooper et al. (2012) suggest using an equivalent monolithic pane of glass to cut processing time. For a 7.52mm laminate construction, the PVB can be removed and the glass is modelled independently as a 6mm ply. This investigates the pre-crack phase by assuming the interlayer has no effect on the behaviour of the laminate as explained by Peng et al. (2013). |

**Table 2: Material models**

The first verification procedure was a mesh convergence study. A refined mesh is important in order to produce a well posed model, this is emphasised by Schwer, Teng and Souli (2015). This study suggests undertaking a mesh convergence study to refine the element size until the results converge irrespective of the accuracy of the results. A sufficiently fine mesh must also be used in order to model the cracks in the plates as these can be very fine.

The structure has been exposed to a uniformly distributed and an exponentially decaying blast load. This can be calculated from the LS-DYNA pre-post using the empirical function LOAD_BLAST_ENHANCED. It is a continuum solver and models a spherical TNT charge in free air with normal temperature and pressure acting on a Lagrangian structure (Hilding, 2016). Equation 2 shows the classical scaling law that is used in this blast formulation:

$$Z = \frac{R}{\sqrt[3]{W}} \tag{2}$$

UFC (2014) have produced graphs such as that seen in appendix B which use equation 2 to calculate the peak and reflected pressures on structures. This has been used alongside experimental data to validate the loading on the specimens. Appendix C shows the blast parameters and corresponding overpressures associated with The Erasmusline. According to

the UFC (2014) guidelines, an important assumption made was that the blast will occur sufficiently close to the floor that a hemispherical blast is produced due to reflection of the incident wave. The loading parameters used for the case study produce a scaled distance of 2.43kg/m$^{1/3}$ (>0.4 kg/m$^{1/3}$) which, according to Han and Liu (2015), can be supported by the LOAD_BLAST_ENHANCED function in LS-DYNA.

Before modelling the case study, a parametric study must be conducted; the format was similar to that conducted by Larcher et al. (2011) where the pre and post-crack behaviour is modelled against experimental results. The parameters used in this study however have been chosen to replicate a non-linear response of the specimen with the honour on shell element formulations and material models. The ultimate aim of this study is to find a method of modelling laminated glass accurately. The vast database of materials, elements, loading, boundary conditions, etc. that is provided by LS-DYNA allows users to construct extensive models that will respond similarly to experiments such as those completed by Kranzer et al. (2005) and Hooper et al. (2012). This study has been carried out by modelling Kranzer et al.'s (2005) experiment to investigate the glass cracking phase of blast loading as well as Hooper et al.'s (2012) blast loaded plate that tests the interlayer to failure, these parameters have then be used to inform the final case study.

**5.0 Theory of shells and its application to glass structure**

The non-linear behaviours of thin shell structures are investigated, especially when exposed to blast. The shell behaviours can be subdivided into component levels. The regimes that can be calculated independently are, the elastic response of the facesheet, elastic response of the core and the elastoplastic respothnse of the core. Further geometrical non-linearities can be included in the model by the correct choice of element formulation; these are applied to the shell elements and allow for a change in stiffness associated with the reduction in element thickness when stretched. The finite element method works by using the force and displacement relationship to calculate the unknown nodal displacements through the production of a global stiffness matrix. This relationship between the forces and displacements at the nodes has been calculated using the virtual work principle.

5.1 Glass Cracking Phase

Kranzer et al. (2005) conducted tests on a 1.1m x 0.9m laminated glass pane with a through thickness construction consisting of a 1.52mm PVB interlayer sandwiched between 2, 3mm glass plies. The glass is held in position by silicone sealant joints which provide elastic boundary conditions; these have been modelled using MAT_024 solid elements. A 0.5kg charge was detonated at a scaled distance of 5.75m to cause cracking of the plies. For the purposes of processing time and power, only 1 quarter of the plate has been modelled. This can be seen in figure 4 and assumes a uniform pressure field across the pane causing symmetry conditions to occur (Hooper et al., 2012). This simplification has also been deployed in models produced by

Hidallana-Gamage et al. (2013), Hooper at al. (2012) and Larcher et al. (2011) which suggest the assumption can be considered valid.
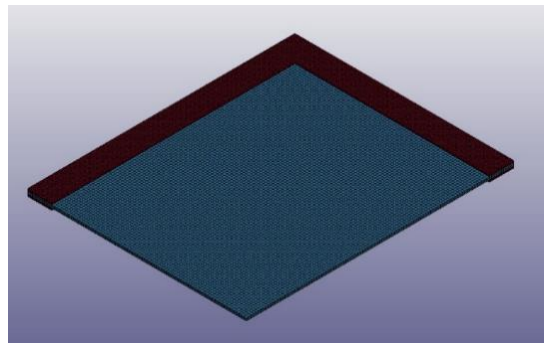


**Figure 4: Finite element model to simplify Kranzer et al. (2005) experiment**

5.2 Interlayer Failure Model

This model is based on an experiment conducted by Hooper et al. (2012) where a 15kg charge was detonated at a scaled distance of 10m causing complete failure of the glass panel and non-linear deflections to be measured. The laminate construction was the same as that conducted by Kranzer et al. (2005) although a larger panel of 1.2m x 1.5m was used. Once again, a quarter of the plate was modelled for computational efficiency however a fixed boundary condition was assumed to ensure the response of the glass (and not the sealant) was analysed. If an elastic boundary was used as in the previous study, very fine meshes would be required to prevent negative volume occurring in each element due to the stronger charge.

The case study has applied the ideal model learnt in the preliminary studies to simulate the breakage configuration of the glass canopy. A repeat of the previous pressure validation has been conducted to ensure the blast pressures are realistic and further potential modes of structural damage has been modelled.

**6.0 Model verification**

6.1 Mesh convergence study

Figure 5 shows the deflection-time history of Kranzer et al.'s (2005) experiment with meshes of varying sizes. It can be seen from this data that a finer mesh produces more of a sporadic response following the rebound. The 2.5mm element size discontinued after around 0.023s, this model was stopped after running for 36hrs due to the instability and failure to converge and will therefore not be carried forward. Despite the coarser meshes producing a smoother oscillation a finer mesh is required to capture the infinitesimal cracking and fragmentation that occurs upon blast. An element size from 5mm to 50mm will therefore be used in these studies in order to capture the full oscillating response of the plate. This is because the stable, converging response can be achieved while the mesh size would not dramatically affect the resolution of crack pattern analysis.

6.2 Blast pressure validation

Figure 6 shows the reflected and incident blast pressures that are experienced by the plate adopted by Kranzer et al. (2005). Table 3 shows the data collected from Kranzer et al (2005), UFC (2014) and the finite element model, to compare the magnitudes of the incident and reflected blast pressures. The table shows that the CONWEP method used by the LOAD_BLAST_ENHANCED function in LS-DYNA provides comparable results with the Friedlander equation (see Equation 2) used in UFC (2014) however underestimates the experimental value by nearly 30%. This loss in pressure could be attributed to the type and size of the charge that was released in Kranzer et al.'s (2005) experiments. In their experiment Kranzer and his co-workers used a PETN explosive whose TNT charge equivalence has been investigated by Hargather and Settles (2007) as well as Kinney and Graham (1985). Both studies postulate that the TNT equivalence of PETN ranges between 0.7 and 1.8 which would produce massive margins in the blast pressures and justify the difference between the model results. For simplicity, an equivalence of 1 has been adopted.

|  | FEM | Kranzer et al. (2005) | UFC (2014) |
|---|---|---|---|
| Incident pressure | 19.67kPa | N/A | 25.00kPa |
| Reflected pressure | 46.07kPa | 65.00kPa | 50.00kPa |

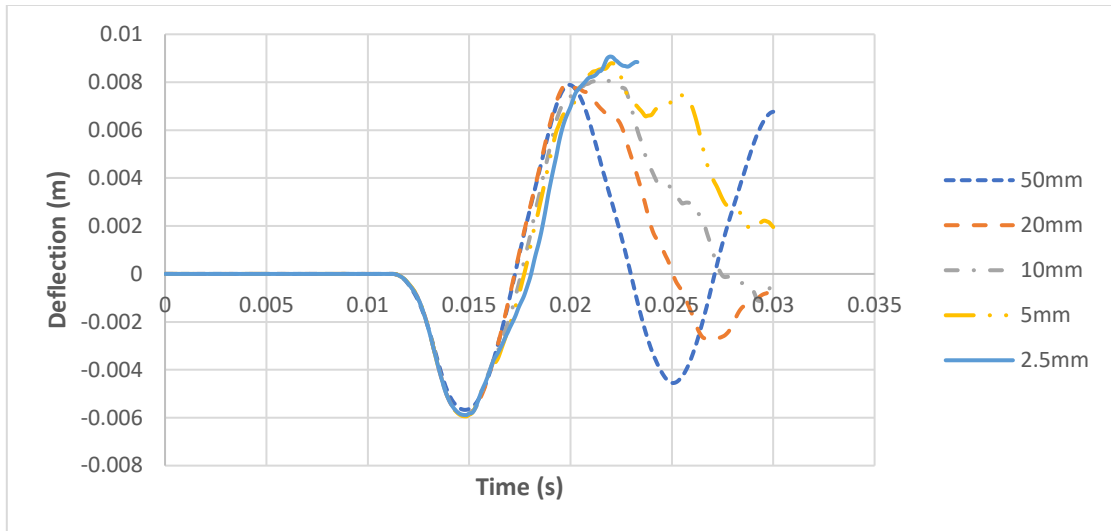**Table 3: Pressure comparison of finite element model**
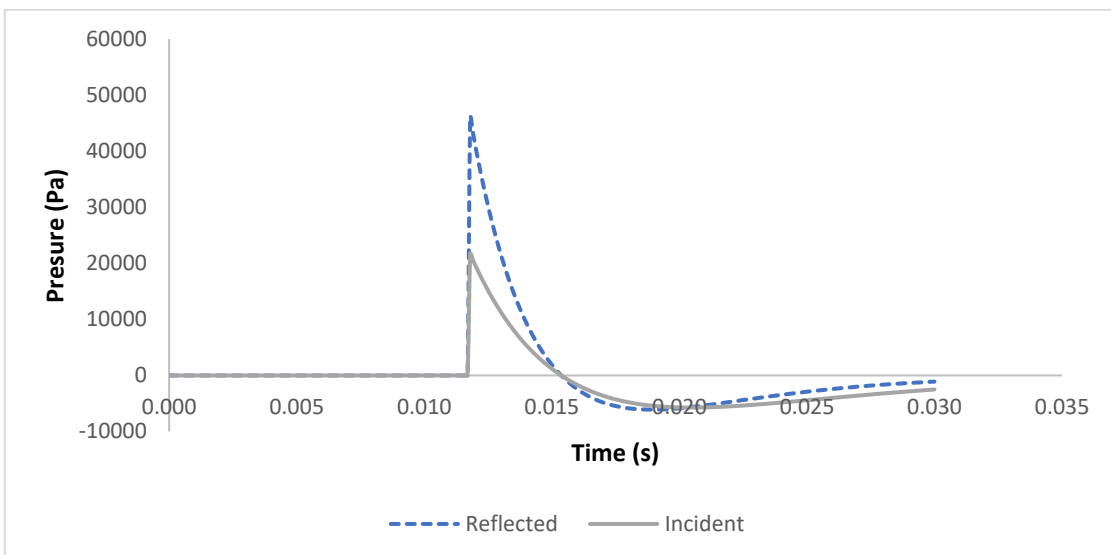
13

**Figure 5: Mesh convergence study**



**Figure 6: Blast pressure data by Kranzer et al. (2005)**
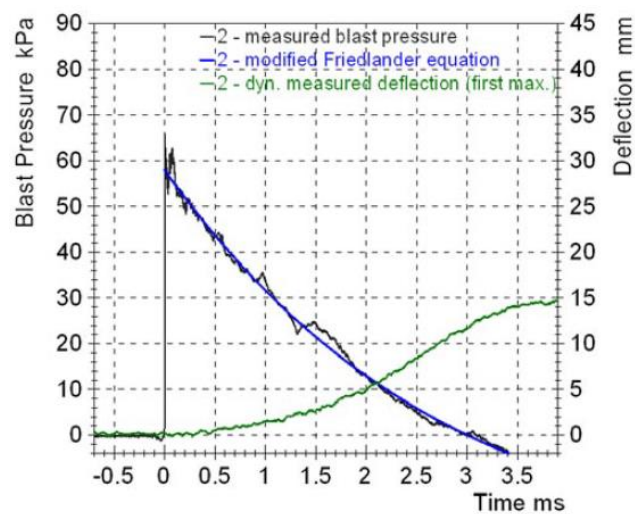


**Figure 7: Kranzer et al. (2005) blast pressure and deflection**

**7.0 Parametric Study**

<u>7.1 Glass cracking models</u>

Figure 7 showed the experimental measurements of the deflection due to blast pressure carried out by Kranzer et al. (2005). Based on the experimental data, Figure 8 demonstrates the deflection-time history of the plate using various material models described in Table 2. These parameters were investigated to identify the material model that closely predicts the composite response of glass panes. From early observation, the time period of the MAT_001 and MAT_110 model is much longer than reality (from tests). This could be attributed to the stiffness of the elastic boundary conditions connected to the glass shells. The material properties of the silicone joint can be found in appendix D and can vary depending on the type of joint used. The stiffness of the specimen does however seem to be effectively modelled with MAT_032, where no difference in time period is measured. This material is able to model the composite efficiency of the laminate and could therefore allow it to replicate the laminate stiffness effectively. This material could prove effective when modelling the case study as it could closely mimic the rigidity of the global structure and its mode of failure.

The results from the finite element models do however seem to show good agreement with experiment, the maximum experimental deflection was measured at 14.9mm (as shown in Figure 7), the most accurate material model in this case is when the plate is modelled as elastic (MAT_001) with a deviation of just 3.36% (as illustrated in Figure 8). This material was included in the model for reasons described by Peng et al. (2013), to investigate whether the pre-crack phase can be modelled elastically. MAT_001 does show good agreement with experimental deflections and therefore could be used with an erosion criterion to delete the element after cracking. This logic has been applied to the post crack model and combined with the solid elements in the following section. The behaviour of this model can be seen in figure 12 as "full construction".

MAT_110 models an equivalent monolithic pane (explained in Table 2) and exhibits a smooth oscillation showing the storage of kinetic energy after the initial deflection leading to increased deflections on rebound as explained by Kranzer et al. (2005). This models the glass response quite effectively with acceptable displacements and time periods on comparison to reality. The difference could be attributed to removal of the interlayer as the cross-sectional moduli will be affected by the thickness of the composite.
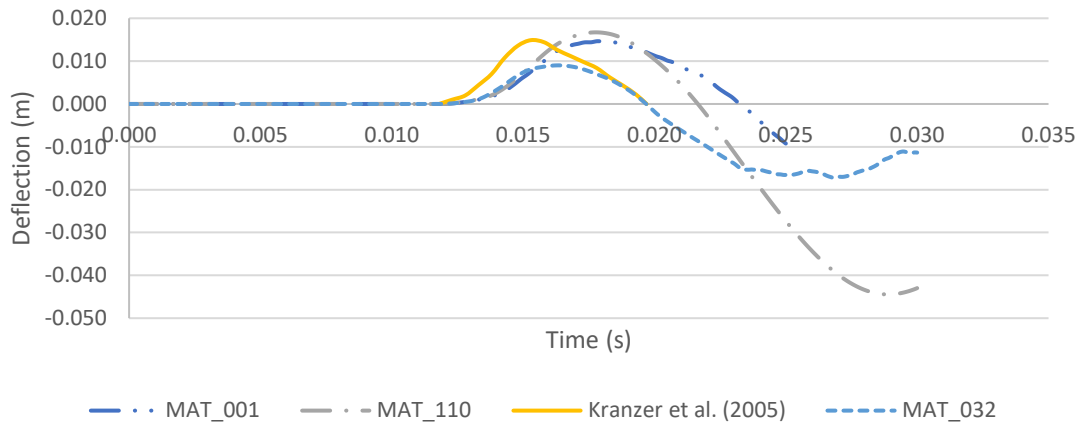
15

**Figure 8: Material parametric study**

| | MAT_001 | | MAT_032 | | MAT_110 | | Experiment (Kranzer et al. (2015) |
|---|---|---|---|---|---|---|---|
| | Value | Percentage difference | Value | Percentage difference | Value | Percentage difference | |
| Initial deflection (mm) | 14.4 | -3.36% | 8.97 | -39.80% | 16.7 | 12.08% | 14.9 |
| Time period (s) | 0.0114 | 44.40% | 0.0079 | 0% | 0.0098 | 24.05% | 0.0079 |

**Table 4: Material model deflection and time period comparison**

7.2 Element Types

The parametric effects of various element formulations or element types can be found in Figure 9. Shell formulations 2 and 16 have very similar responses until 0.0275s where ELFORM 2 (Belytschko-Tsay shell**)** destabilises. Stelzmann, (2010) attributes this phenomenon to the lack of integration points (2) in plane which produce warping instabilities due to excessive shear deformations. ELFORM 16 however is a fully integrated shell that remains stable throughout the simulation, this is ideal for non-linear analysis as the shell stiffness will change with deformation, it is however 2-3 times more expensive than the Belytschko-Tsay shell (Stelzmann, 2010). This improved robustness leads to the Belytschko-Tsay shell being the solver's default element formulation.

As shown in Table 5, TSHELLs are used if the neutral axis is able to move throughout bending (Haufe, Schweizerhof and DuBois, 2013), this phenomenon occurs as the strength is lost in each ply due to cracking. MAT_LAMINATED_GLASS (MAT_032) has been used for this study and shows good accuracy in the initial deflection of the glass pane, especially ELFORM 2 with only a 0.67% difference in the mid surface displacement. These elements however show a much slower rebound with the time period difference of TSHELL ELFORM 2 reaching 259.5%.

16

This slower response could be associated with their compatibility with a user defined integration rule through the thickness that assumes every integration point occupies an equal spacing. This is not the case especially when the glass plies are much thicker than the interlayer.
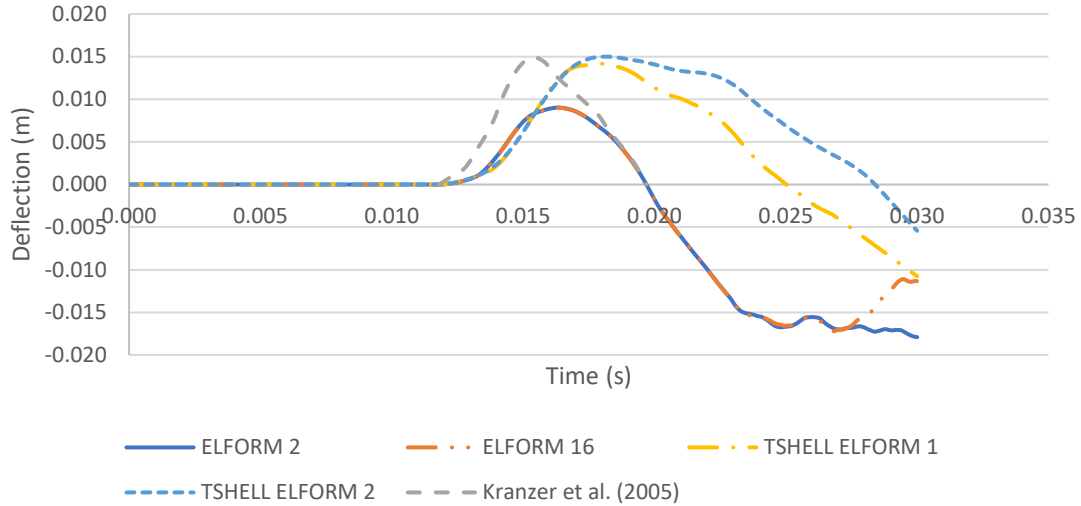


**Figure 9: Element formulation parametric study**

| | ELFORM 2 | | ELFORM 16 | | TSHELL ELFORM 1 | | TSHELL ELFORM 2 | | Experiment |
|---|---|---|---|---|---|---|---|---|---|
| | Value | Percentage difference | Value | Percentage difference | Value | Percentage difference | Value | Percentage difference | Kranzer et al. (2005) |
| Initial deflection (mm) | 8.97 | -39.80% | 8.97 | -39.80% | 14.1 | -5.36% | 15.0 | 0.67% | 14.9 |
| Time period (s) | 0.0079 | 0% | 0.0079 | 0% | 0.0132 | 67.1% | 0.0284 | 259.5% | 0.0079 |

**Table 5: Blast effects on deflection and time period under various element types**

<u>7.3 Cracked Pattern</u>

This study has been used to illustrate the accuracy of the finite element model by highlighting the areas (in red) where the failure strain of glass has been exceeded. This informs the user about the adequacy of the boundary conditions through the distribution of cracks compared to the experiment. The failure strain of 0.001 was suggested by Larcher et al. (2011) who emphasised caution with this parameter due to its sensitivity in the model. The finite element model and experiment crack pattern can be found in Figures 10 and 11. This model used MAT_032, due to its failure algorithm mentioned in Table 2, which shows similar stress wave redistribution to the damage found in experimental results. A potential reason for the lack of cracking in the centre of the finite element model could be attributed to the size of the cracks that formed in the specimen. The element size remained at 5mm for this study as explained in the mesh convergence study. This mesh is too coarse to model these infinitesimal cracks at the centre hence no plastic strains were computed. Furthermore, the lack of cracking in the centre

of the finite element model could potentially be attibuted to excessive deflections of the larger cracks around the outside which relieve the stress on the inner elements. This has not occurred in Kranzer et al.'s (2005) specimen as micro-cracks are still able to withstand some stresses to transfer to the centre elements. To enable detailed crack analysis, a separate uncoupled glass model should be used to avoid global finite element divergence. In this study, the optimal mesh of 5 mm will be focused to enable the analysis of coupling models between glass and long-span structures.



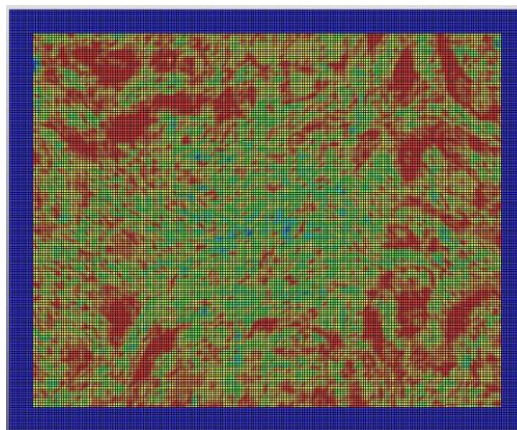**Figure 10: Kranzer et al. (2005) cracked specimen**



**Figure 11: Finite element model cracked glass distribution**

7.4 Interlayer failure model, Hooper et al. (2012)

From the previous study (as illustrated in Figure 12), it can be concluded that fully integrated shell element 16 shows a more stable response when non-linear deflections exist and hence will be used in these studies. The parameters investigated in this study can be seen in Figure 12. There is no rebound of the plate in this experiment as the blast impulse is too powerful causing the glass to crack and lose all energy as heat thus preventing the glass from springing

back. This was postulated by Peng et al. (2013), and states the response is now a function of the interlayer which behaves under a non-linear elastoplastic regime when exposed to rapid strain rates such as that from blast. The models tested show a healthy variation of responses surrounding that of the experiment with shell elements showing a slower deflection rate and solid elements more rapid deflections.

This disparity between the shell element model and experiment is potentially a result of the shear stress distribution through the thickness of the laminate. The pre-crack response shows good agreement to experiment as the shear stress distribution in the uncracked laminate is co-linear (similarly in Figure 1a) and the composite reacts elastically. These elastic results are commonly found. Once cracking occurs, hyperelastic deformations of the interlayer complicate the finite element response. The more rapid deflections of the experiment could be associated with the extent of micro-flaws across the pane which are pre-instilled during the production process, this is explained by Zhang, Hao and Ma. (2013), who stated that the strength of glass specimens follow a Weibull distribution, thus making material properties hard to control. Furthermore, tests conducted by Zhang et al., (2012) show a relaxation in the modulus of glass before fracture, these phenomena cannot be modelled by LS-DYNA and could therefore contribute to the disparity in results.

Failure of the plate tested by Hooper et al. (2012) can be seen propagating from the boundary where the specimen is fixed. This mode of failure is characteristically shear force induced due to the rapid, intense pressure impulse causing cracking initiating at the boundaries (Zhang, Hao and Ma, 2013). The fixed boundary conditions pose a more conservative model than the elastic support used previously. Greater stresses are experienced in the perimeter elements causing premature failure. This theory is supported by Figure 13 by showing the plastic strains in the model. This shows well posed model as a similar response is seen in the experiment whereby the very high strains are experienced at the boundaries and the central region is largely undeformed.

In keeping with Hooper et al.'s (2012) recommendations and to control processing times, an equivalent monolithic pane of solid elements (MAT_110) was adopted. This reduced cross-sectional depth would therefore reduce the strength of the panel in bending due to the parallel axis theorem thus leading to greater bending rates shown in this study. These results can be rectified by introducing the interlayer as solid elements to maintain that separation and improve the flexural stiffness. MAT_LINEAR_PIECEWISE_PLASTICITY has been used extensively in open literature to simulate the elastoplastic response and has been implemented in this study. The glass plies were simulated as simple elastic shells with a predefined failure criteria used previously. The more complex behaviour of PVB is captured by solid elements allowing shear transfer between the plies and improve flexural stiffness through the parallel axis theorem. This model shows a better response than the monolithic pane however still showing a steeper

deflection rate than experiment. Zhang et al., (2012) suggest using a dynamic increase factor (DIF) of 1.7 that accounts for the strain rate effects on the yield strength, this would have a positive effect on the results and prevent premature deletion.

Hooper et al. (2012) time 9ms for the interlayer to tear at the boundaries. In the finite element model the perimeter elements started eroding from 4ms. This premature failure is most likely associated with the failure criterion used in the model. Hidallana-Gamage et al. (2017) suggest using a strain to failure of 200%. Studies conducted by Zhang et al. (2013) suggest a hyperelastic material law could be even adopted as strains in the interlayer can reach up to 300%. This further explains the difficulties in using erosion criteria to model composites especially in those like laminated glass where their properties are very poorly defined.
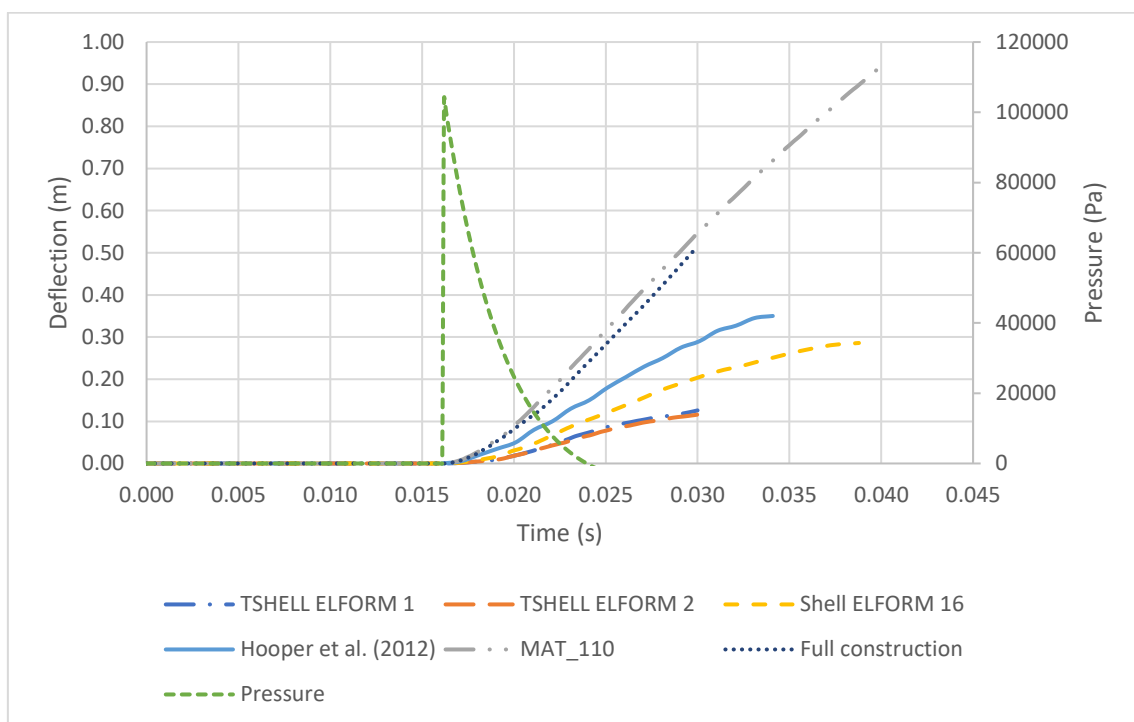


**Figure 12: Parametric effects of material models vs experiments by Hooper et al. (2012)**
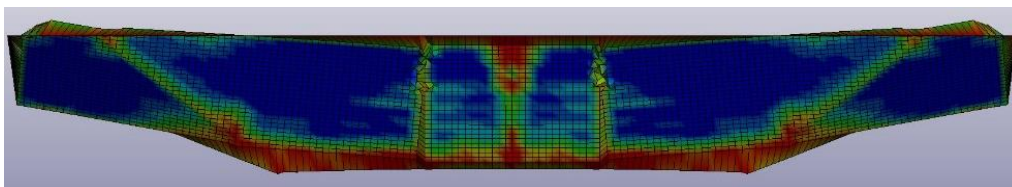


**Figure 13: Finite element model side view of deformed shape and cracked glass**

## 8.0 Case study

In comparison to the glass panels that were modelled in the preliminary studies, the scale of the structure is much larger as shown in Figure 14. The suitable material models and element type from the previous parametric study has been adopted in the modelling for this case study. The explosion scenario is chosen based on the potentially maximum response. The explosive device is installed at the middle of the concourse (at the screen door gates – as tabulated in Appendix C). In this full-scale model, this immediately proves to be problematic when meshing the 90m long canopy. The 5mm meshes used previously have been increased to 50mm producing 766855 shell elements and 970907 nodes. This mesh size and density was chosen to allow the model to generate a comparable eigenfrequency similar to that of blast as coarse meshes do not contain sufficient degrees of freedom. The size of these elements mean that cracks can no longer be modelled however the breakage configuration is more suited and hence why a Von-Mises stress alike Kaewunruen et al., (2017) has been used to show this damage evolution better. For processing efficiency, the shell model MAT_LAMINATED_GLASS with element formulation 16 has been used to identify where the failure strains occur as well as reduce processing time. This formulation has proven effective when modelling the crack distribution as well as the time period of oscillation (as shown in Appendix E). The excited modes of vibration that the structure will exhibit can therefore be simulated with confidence due to similar global rigidities. The mode of vibration is found to be reasonable for the large-span structure.

Figure 14 shows no damage to the upper canopy as the structure can be seen to flex and dissipate the blast flux as heat and kinetic energy. It does however show stress concentrations at the fully pinned supports. The translational restraint provided by these joints cause glass cracking and potential detachment. This model can therefore inform another verification study to check whether the most heavily loaded glass pane will exhibit full interlayer failure and exit the structure or remain attached to the steel gridshell. The doubly curved, laminated glass panel can be seen in Figure 15. It uses the "full construction" model as seen in Figure 12 and supports the full structure model results by confirming that no fragmentation or detachment occurs around the upper canopy. Figure 16 shows that the principal strains in the glass ply are an order of magnitude smaller than its failure strain and hence no cracking is observed. This blast resistance can be fully attributed to the improved sectional moduli associated with this increased thickness of construction.

So far, explicit analysis has modelled the forced vibration stage of structural displacement; the short duration of blast produces local vibrations to the glass canopy. Global modes of vibration will also occur and can be calculated through eigenvalue analysis. Implicit analysis has been conducted to find this mode. The first and most destructive mode can be seen in appendix E (stimulated over a computation time period of 1065s to enable complete modal responses), where the structure resonates at its natural frequency. The dynamic displacements produced can exceed 3m at the open end. The excited vibrations that are stimulated by the blast impulse

however take a much higher modal frequency that occurs around time periods in the region of 10ms (100Hz). These modes can only be simulated by increasing the number of degrees of freedom which make models very expensive to run. Figure 16 shows the excitation of the canopy around 20Hz. Unfortunately, the solver was unable to calculate modes greater than 20Hz however the vibrations can be considered much more local than the resonant frequency. With increasing frequencies, responses will become more local, deflections will become less violent and damage would not be as catastrophic.

An assumption made in this model is that the glass canopy has been simplified to be a continuous surface. By parametric studies, the mesh and boundary condition has been set to enable reasonable structural behaviours. Figure 17 shows a steel gridshell structure that supports the curved glass panels. This level of detail would generate too many inaccuracies due to the inclusion of slender elements like steel which complicate the model. This simplification will mean the bending stiffness of the entire stricture will rely on the material and sectional properties of the glass and the support conditions. The change in mass associated with the inclusion of the steel grid shell has been assumed sufficiently small to not affect the modal response of the canopy. In addition, the slenderness of the steel members have been assumed to be negligible compared to that of glass to ensure that the global stiffness of the structure is a function of the glass and not the steel. It can be observed that a very brief eigenvalue analysis has been conducted on this study mainly to inform future work on the modes of vibration associated with this structure. Further modelling is recommended to identify the localised effects on the dynamic responses. The better insight of the dynamic responses under various worse-case scenarios will help engineers to make appropriate decision for structural retrofitting against the attacks and for disaster and crisis recovery by better identification of failure modes, crack severity, and other potential risks.
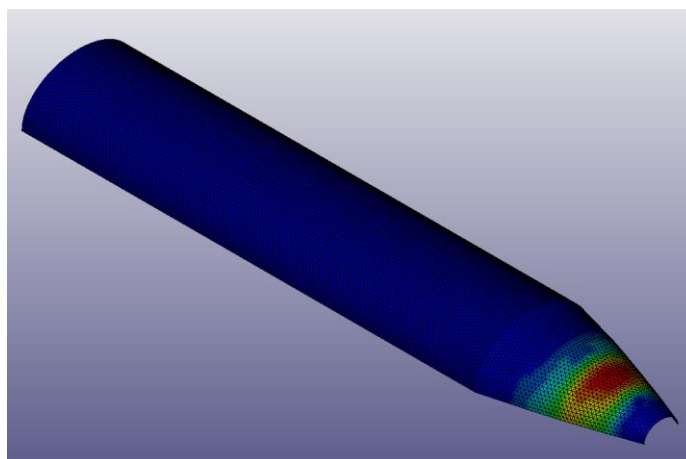


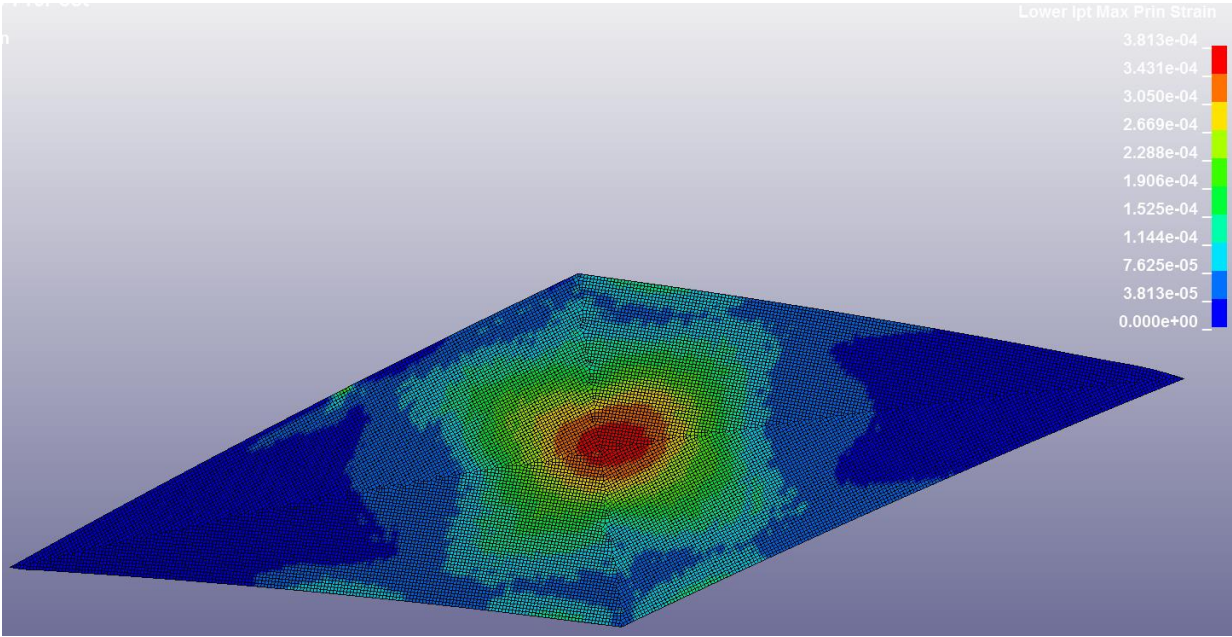**Figure 14: The Erasmusline Von-Mises stress evolution**

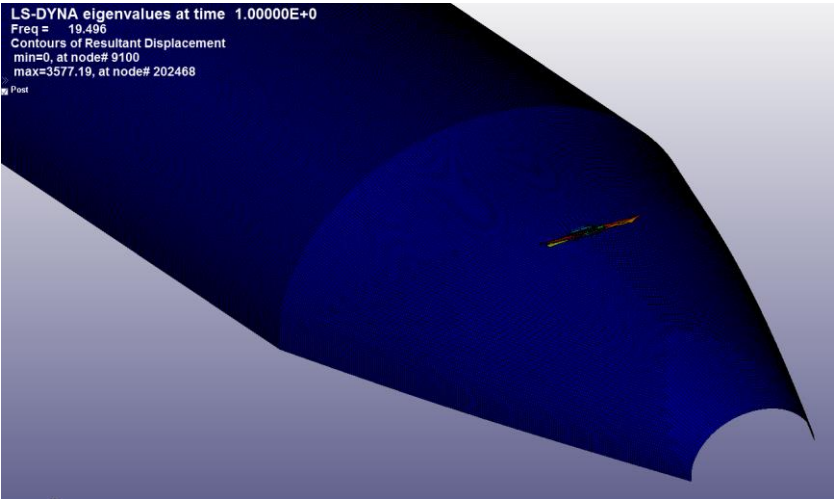**Figure 15: Principal strains in laminated glass panel removed from structure (no fracture)**



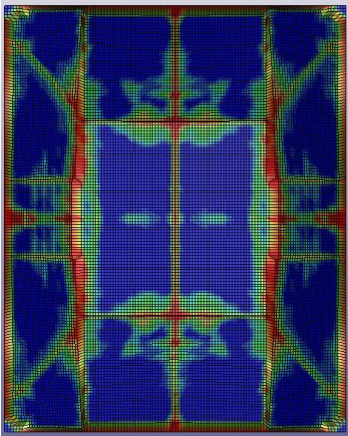**Figure 16: 20Hz Eigenfrequency excitation**

**Figure 17: Finite element model plan view of cracked glass distribution – Hooper et al. (2012) experiment**

## 9.0 Conclusions

This research investigated the blast effects on highly non-linear, thin shell structures, through a rigorous parametric study to identify the suitable material non-linearities, as well as an effective model of a light rail station in The Netherlands to model the geometric non-linearities of its roof canopy. The study has critically reviewed and established a suitable model for the non-linearities of laminated glass shell structures. Experiments conducted by Kranzer et al. (2005) and Hooper et al. (2012) have been reconstructed using finite element codes in LS-DYNA. Each experiment tests laminated glass panels against blast to investigate the different stages of failure of the composite.

These models are able to effectively represent the pre-crack phase of glass deflection through the inexpensive, fully integrated, shell formulation 16 and material model 32. The shell model subsequently reacted stiffer than the experiment when modelling the post-crack phase. The opposite response occurred when the full laminate construction was modelled using both shell and solid elements in attempt to model the differential shear deformations across the laminate. Erosion criteria assigned to each layer proved to lead to premature deletion from the modal and hence greater deflections. The models proven to be effective in the parametric study were subsequently used when investigating the response of the case study to a 15kg blast. The breakage configuration was investigated and found stress concentrations located at the fully pinned supports causing cracking. To validate the full structural model, the most heavily loaded pane was removed and loaded independently showing no cracking. Finally, the eigenfrequencies associated with blast loading have been investigated to check for any further damage related to the global impulsive excitation from the blast.

Future work includes an efficient simulation of the blast wave by meshing the entire domain, which enables wave reflection and superposition to be captured. Wave reinforcement phenomena have the potential to cause much more damage than the initial overpressures and therefore must be accounted for. Detailed structural member and joint analyses will be considered. Functions such as MM-ALE solver or smooth particle hydrodynamics are suggested by Schwer, Teng and Souli (2015) can aid model validation.

24

## References

Blaauwendraad, J. and Hoefakker, J. (2014). *Structural shell analysis*. Dordrecht: Springer.

Bohm, R., Haufe, A. and Erhart, A. (2016). A Novel Approach to Model Laminated Glass. [online] Stuttgart: DYNAmore. Available at: https://www.dynamore.de/de/download/papers/2016-ls-dyna-forum/Papers%202016/dienstag-11.10.16/materials-and-simulations/novel-approach-to-model-laminated-glass [Accessed 16 Mar. 2018].

British Gas Corporation (n.d.). THE RESPONSE OF GLASS WINDOWS TO EXPLOSION PRESSURES. I. CHEM. E. SYMPOSIUM SERIES. [online] Available at: https://www.icheme.org/communities/subject_groups/safety%20and%20loss%20prevention/res ources/hazards%20archive/~/media/Documents/Subject%20Groups/Safety_Loss_Prevention/H azards%20Archive/VI/VI-Paper-10.pdf [Accessed 16 Jan. 2018].

Chang, T. and Sawamiphakdi, K. (1981). Large deformation analysis of laminated shells by ftnife element method. *Computers & Structures*, 13(1-3), pp.331-340.
Cormie, D., Mays, G. and Smith, P. (2009). *Blast effects on buildings*. London: Thomas Telford Ltd.

Coskun, E. (2016). *Structural Systems*.

Cronin, D., Bui, K., Kaufmann, C., McIntosh, G. and Berstad, T. (n.d.). Implementation and validation of the Johnson-Holmquist ceramic model in LS-DYNA. In: *LS-DYNA users cpmference*.

Deng, R. and Jin, X. (2010). Numerical Simulation for Blast Analysis of Insulating Glass in a Curtain Wall. *International Journal for Computational Methods in Engineering Science and Mechanics*, [online] 11(3), pp.162-171. Available at: http://www.tandfonline.com/doi/full/10.1080/15502281003702302?scroll=top&needAccess=true &instName=University+of+Birmingham [Accessed 30 Nov. 2017].

Dharani, L. and Wei, J. (2004). Dynamic response of laminated glass under blast loading: effect of negative phase. In: N. Jones, ed., *Structures under shock and impact*, 8th ed. [online] Missouri: WIT Press. Available at: http://www.witpress.com [Accessed 21 Nov. 2017].

25

Fam, A. and Rizkalla, S. (2006). Structural performance of laminated and unlaminated tempered glass under monotonic transverse loading. *Construction and Building Materials*, 20(9), pp.761-768.

Flickr. (2017). *M*. [online] Available at: https://www.flickr.com/photos/95706850@N04/34114137246/ [Accessed 24 Nov. 2017].

Gibson, J. (1980). *Thin shells*. Oxford [u.a.]: Pergamon Pr.

Han, Y. and Liu, H. (2015). Finite Element Simulation of Medium-Range Blast Loading Using LS-DYNA. *Shock and Vibration*, [online] 2015, pp.1-9. Available at: https://www.hindawi.com/journals/sv/2015/631493/ [Accessed 28 Mar. 2017].

Hargather, M. and Settles, G. (2007). Optical measurement and scaling of blasts from gram-range explosive charges. *Shock Waves*, 17(4), pp.215-223.

Haufe, A., Schweizerhof, K. and DuBois, P. (2013). Properties & Limits: Review of Shell Element Formulations. In: *Developer Forum*. [online] Available at: https://www.dynamore.de/de/download/papers/2013-ls-dyna-forum/documents/review-of-shell-element-formulations-in-ls-dyna-properties-limits-advantages-disadvantages [Accessed 13 Mar. 2018].

Helbig, T., Kamp, F., Schieber, R., Oppe, M., Torsing, R. and Kieft, R. (2016). Double-layer curved steel-structure with bent glazing New Departure Station Erasmusline, The Hague (NL). In: *Conference on Architectural and Structural Applications of Glass*. [online] The Hague: Challenging Glass 5. Available at: http://www.zja.nl/en/media/inline/id/4069 [Accessed 24 Nov. 2017].

Hidallana-Gamage, H., Thambiratnam, D. and Perera, N. (2013). Computational Analysis of Laminated Glass Panels Under Blast Loads: A Comparison Of Two Dimensional And Three Dimensional Modelling Approaches. *The International Journal Of Engineering And Science (IJES)*, 2(8), pp.69-79.

Hidallana-Gamage, H., Thambiratnam, D. and Perera, N. (2014). Failure analysis of laminated glass panels subjected to blast loads. *Engineering Failure Analysis*, [online] 36, pp.14-29. Available at: http://www.sciencedirect.com/science?_ob=ArticleListURL&_method=list&_ArticleListID=-1242386575&_sort=v&_st=17&view=c&_origin=related_art&panel=citeRelatedArt&_mlktType=Journal&md5=5ff213c210d742157b4249cc11413323&searchtype=a [Accessed 15 Nov. 2017].

Hidallana-Gamage, H., Thambiratnam, D. and Perera, N. (2017). Influence of the negative phase and support flexibility on the blast response of laminated glass panels. *Construction and Building Materials*, 154, pp.462-481.

Hilding, D. (2016). *Methods for Modelling Air Blasts on Structure Using LS-DYNA*.

Hoo Fatt, M. and Sirivolu, D. (2015). Blast response of double curvature, composite sandwich shallow shells. *Engineering Structures*, 100, pp.696-706.

Hooper, P., Sukhram, R., Blackman, B. and Dear, J. (2012). On the blast resistance of laminated glass. *International Journal of Solids and Structures*, 49(6), pp.899-918.

Karlos, V. and Solomos, G. (2013). *Calculation of Blast Loads for Application to Structural Components*. [online] Joint Research Centre. Available at: http://publications.jrc.ec.europa.eu/repository/bitstream/JRC87200/lbna26456enn.pdf [Accessed 22 Mar. 2018].

Kaewunruen, S., Pompeo, G. and Bartoli, G. (2017). BLAST SIMULATIONS AND TRANSIENT RESPONSES OF LONGSPAN GLASS ROOF STRUCTURES: A CASE OF LONDON'S RAILWAY STATION. In: *UKACM Conference on Computational Mechanics*. [online] Birmingham: Be Press. Available at: https://works.bepress.com/sakdirat_kaewunruen/83/ [Accessed 20 Nov. 2017].

Kinney, G. and Graham, K. (1985). *Explosive Shocks in Air*. New York: Springer.

Kranzer, C., Gurke, G. and Mayrhofer, C. (2005). Testing of Bomb Resistant Glazing Systems: Experimental Investigation of the Time Dependent Deflection of Blast Loaded. *Glass Processing Days*.

Larcher, M., Forsberg, R., Björnstig, U., Holgersson, A. and Solomos, G. (2015). Effectiveness of finite-element modelling of damage and injuries for explosions inside trains. *Journal of Transportation Safety & Security*, 8(sup1), pp.83-100.

Larcher, M., Solomos, G., Casadei, F. and Gebbeken, N. (2011). Experimental and numerical investigations of laminated glass subjected to blast loading. *International Journal of Impact Engineering*, 39(1), pp.42-50.

Larcher, M., Teich, M., Gebbeken, N., Solomos, G., Casadei, F., Falcon, G. and Sarmiento, S. (2011). Simulation of Laminated Glass Loaded by Air Blast Waves. *Applied Mechanics and Materials*, 82, pp.69-74.

Li, R., Kardomateas, G. and Simitses, G. (2008). Nonlinear Response of a Shallow Sandwich Shell With Compressible Core to Blast Loading. *Journal of Applied Mechanics*, 75(6), p.061023.

Mollmann, H. (1981). *Introduction to the theory of thin shells*. Chichester: Wiley.

National Consortium for the Study of Terrorism and Responses to Terrorism (2016). *Terrorist Attacks Targeting Critical Infrastructure in the United States, 1970-2015*. [online] Maryland: START. Available at: https://www.start.umd.edu/pubs/DHS_I%26A_GTD_Targeting%20Critical%20Infrastructure%20in%20the%20US_June2016.pdf [Accessed 22 Mar. 2018].

Ngo, T., Mendis, P., Gupta, A. and Ramsay, J. (2007). Blast Loading and Blast Effects on Structures – An Overview. *EJSE- Loading on Structures*. [online] Available at: http://www.ejse.org/Archives/Fulltext/2007/Special/200707.pdf [Accessed 19 Jan. 2018].

Pelfrene, J., Kuntsche, J., Van Dam, S., Van Paepegem, W. and Schneider, J. (2016). Critical assessment of the post-breakage performance of blast loaded laminated glazing: Experiments and simulations. International Journal of Impact Engineering, 88, pp.61-71.

Peng, Y., Yang, J., Deck, C. and Willinger, R. (2013). Finite element modeling of crash test behavior for windshield laminated glass. *International Journal of Impact Engineering*, 57, pp.27-35.

Schwer, L., Teng, H. and Souli, M. (2015). LS Dyna blast techniques: Comparisons for experiments for close in charges. In: *European LS-DYNA Conference*. DYNAmore GmbH.

Stelzmann, U. (2010). die große element bibliothek in ls dyna. In: *ANSYS conference and 28th CADFEM Users' Meeting*. [online] CADFEM. Available at: http://www1.beuth-hochschule.de/~kleinsch/Expl_FEM/2010_Elementbibliothek_LSDyna_Cadfem.pdf [Accessed 13 Mar. 2018].

Subramani, T. and Sugathan, A. (2012). Finite Element Analysis of Thin Walled-Shell Structures by ANSYS and LS-DYNA. *International Journal of Modern Engineering Research (IJMER)*, 2(4).

Ter Maten, R. (2011). *Ultra High Performance Concrete in Large Span Shell Structures*. Undergraduate. Delft University of Technology.

Unified Facilities Criteria (UFC) 2014 *Structures to Resist the Effects of Accidental Explosions, U. S. Army Corps of Engineers*, Naval Facilities Engineering Command, Air Force Civil Engineer Support Agency, UFC 3-340-02, 5 December 2014.

Zhang, X., Hao, H. and Ma, G. (2013). Parametric study of laminated glass window response to blast loads. *Engineering Structures*, 56, pp.1707-1717.

Zhang, X., Zou, Y., Hao, H., Li, X., Ma, G. and Liu, K. (2012). Laboratory Test on Dynamic Material Properties of Annealed Float Glass. *International Journal of Protective Structures*, 3(4), pp.407-430.

Zhang, X., Zou, Y., Hao, H., Li, X., Ma, G. and Liu, K. (2012). Laboratory Test on Dynamic Material Properties of Annealed Float Glass. *International Journal of Protective Structures*, [online] 3(4), pp.407-430. Available at: http://journals.sagepub.com/doi/abs/10.1260/2041-4196.3.4.407 [Accessed 14 Mar. 2018].

**Appendix A: Johnson Holmquist Ceramics parameters for glass (Hidallana-Gamage, Thambiratnam and Perera, 2017)**

| Material property/JH–2 constant | Value |
| --- | --- |
| Density ($\rho$) | 2530 kg/m$^3$ |
| Young's modulus (E) | 72 GPa |
| Poisson's ratio ($\upsilon$) | 0.22 |
| *Strength constants* | |
| A | 0.93 |
| B | 0.2 |
| C | 0.003 |
| M | 1.0 |
| N | 0.77 |
| Ref strain rate (EPSI) | 1.0 |
| Tensile strength (T) | 60 MPa |
| Failure strain | 0.0024 |
| Normalized fractured strength | 0.5 |
| HEL | 5.95 GPa |
| HEL pressure | 2.92 GPa |
| HEL strength | 4.5 GPa |
| *Damage constants* | |
| D1 | 0.043 |
| D2 | 0.85 |
| *Equation of state* | |
| K1 (bulk modulus) | 45.4 GPa |
| K2 | −138 GPa |
| K3 | 290 GPa |
| $\beta$ | 1.0 |

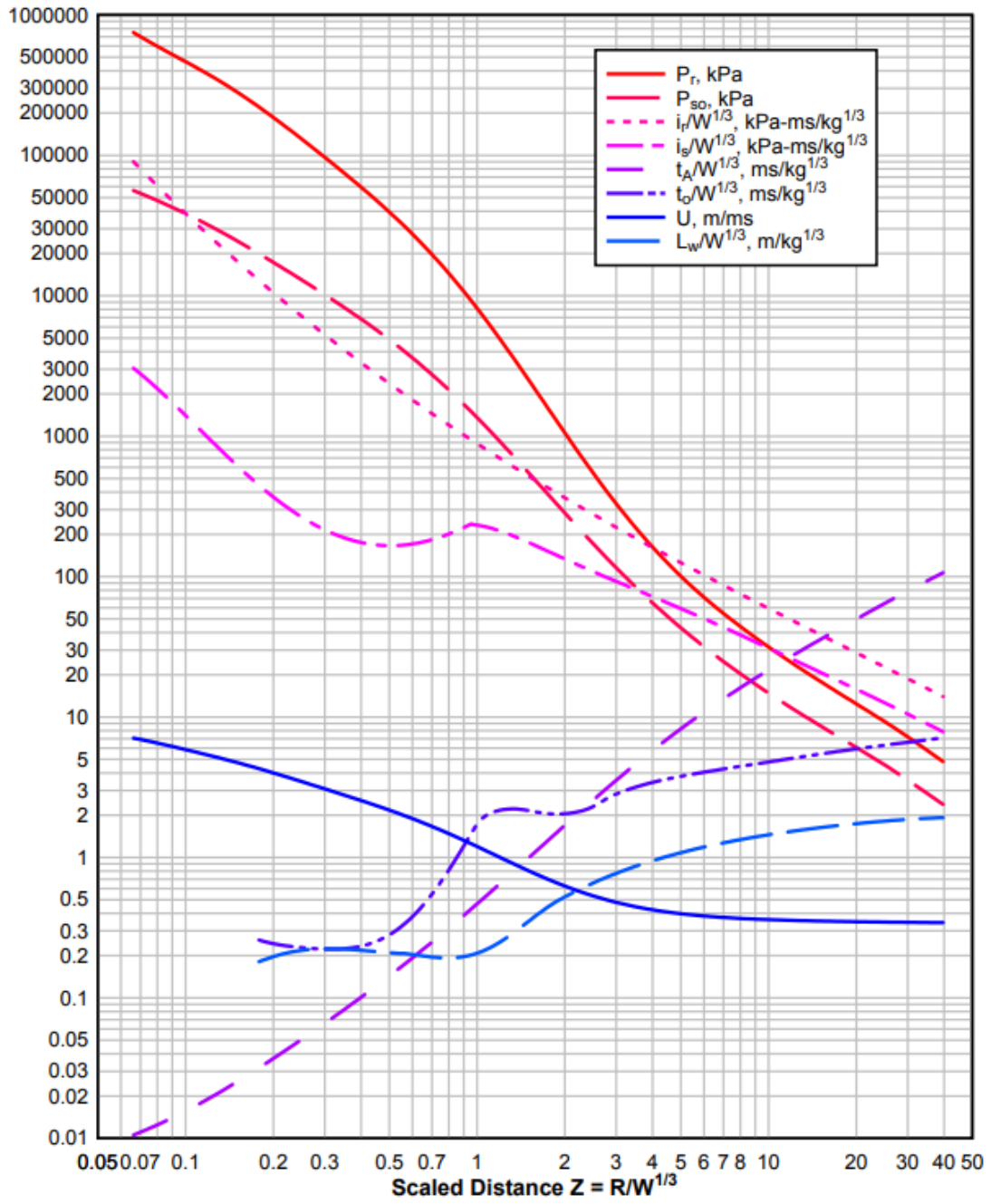## Appendix B – Hemispherical blast load response



**Figure 18: Hemispherical blast load response (Karlos and Solomos, 2013)**

**Appendix C – Charge parameters and corresponding overpressures according to UFC (2014)**

|  | Kranzer et al. (2005) | Hooper et al. (2012) | Erasmusline |
|---|---|---|---|
| Stand-off distance (m) | 5.75 | 10 | 6 |
| Charge weight (kg) | 0.5 | 15 | 15 |
| Scaled distance | 7.24 | 4.05 | 2.43 |
| Reflected pressure (kPa) | 50 | 150 | 700 |
| Incident pressure (kPa) | 25 | 60 | 220 |

**\* Charge parameters used in equation 2**

**Appendix D: Material properties of PVB and Silicone**

| Material property | PVB | Rubber |
|---|---|---|
| Density ($\rho$) | 1100 kg/m$^3$ | 1100 kg/m$^3$ |
| Young's modulus (E) | 530 MPa | 2.3 MPa |
| Poisson's ratio ($\upsilon$) | 0.485 | 0.495 |
| Yield stress | 11 MPa | 2.3 MPa |
| Ultimate stress | 28 MPa | 3.5 MPa |
| Failure stress | 28 MPa | 3.5 MPa |
| Failure strain | 2 | 2.5 |

Table 6: Material properties of PVB and silicone (Hidallana-Gamage, Thambiratnam and Perera, 2017)
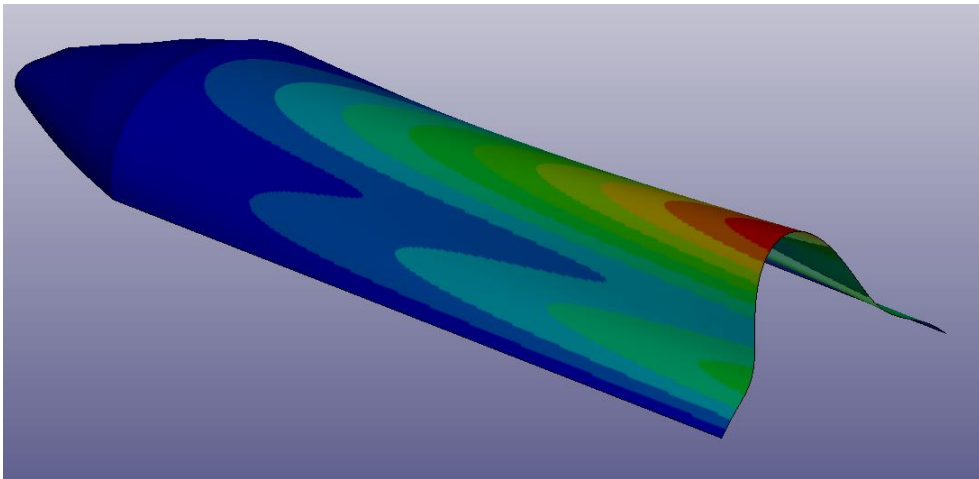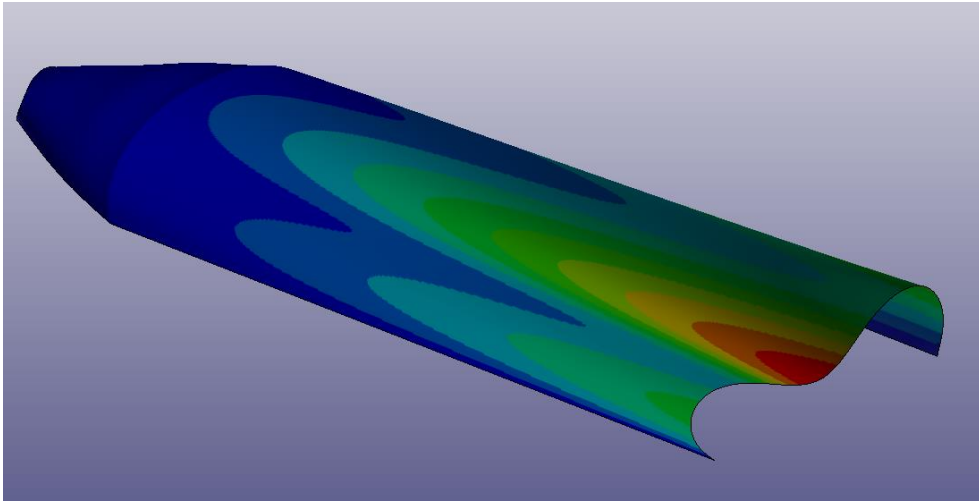
**Appendix E: 1st modal frequency of Erasmusline**



Figure 19: Resonant frequency of The Erasmusline